COST Meeting, Lyon, 17 Nov. 2014

Polynomial fits for CompOSE

F. Burgio (INFN Catania)

M. Baldo, F. B., H.-J. Schulze, G. Taranto (INFN Catania)
D. P. Zhang, Z. H. Li (Fudan Univ., Shanghai)
A. Li, X. R. Zhou (Xiamen Univ.)
T. Rijken (Nijmegen Univ.)

The Bethe-Goldstone equation for the G-matrix :

$$G(\rho;\omega) = V + \sum_{k_a,k_b} V \frac{|k_a k_b > Q < k_a k_b|}{\omega - e(k_a) - e(k_b)} G(\rho;\omega)$$

$$e(k;\rho) = \frac{k^2}{2m} + U(k;\rho)$$

$$U(k;\rho) = Re \sum_{k' \leq k_F} < kk'|G(\rho:\omega)|kk' >$$

Results : energy density, effective masses .....

$$\epsilon = \sum_{N=n,p} \frac{1}{\pi^2} \int_0^{k_F^{(N)}} dk\ k^2 \left(\frac{k^2}{2m_N} + \frac{1}{2} U_N(k) \right)$$

$$\frac{m^*(k;\rho)}{m} = \frac{k}{m} \left[\frac{de(k;\rho)}{dk} \right]^{-1}$$

✓Self-consistent and parameter free procedure.

✓The only input required is the NN potential V.

BUT

Problem : wrong saturation point.

Solution : Inclusion of three-body forces (TBF's).

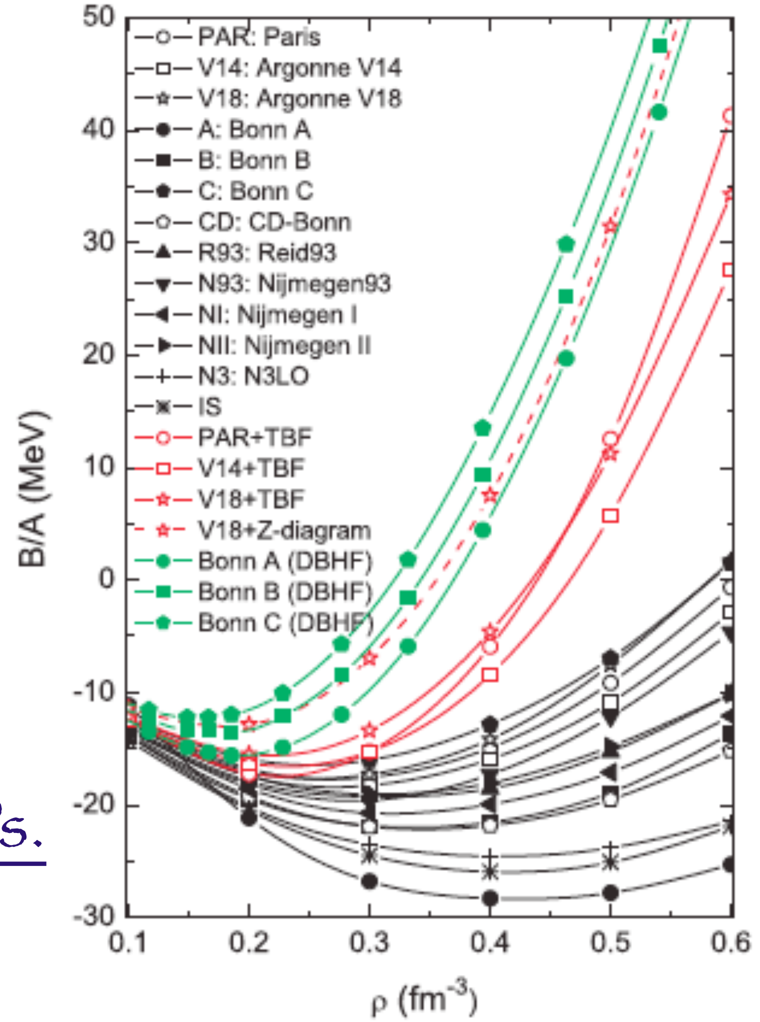

Fits calculated for several choices of NN potentials and TBF's.

- Symmetric (SNM) and purely neutron (PNM) matter
- Easily extended to asymmetric matter using the parabolic approximation

$$\frac{B}{A}(\rho, x_p) = \frac{B}{A}(\rho, x_p = 0.5) + E_{sym}(\rho)(1 - 2x_p)^2$$

Case a) : T=0

- G and K matrices
- NN potentials : Argonne v18, Bonn B, Njimegen 93, CD Bonn
- TBF : Urbana IX (Pudliner et al. 1995) and Microscopic (Grangè et al. 1989)

$$\Rightarrow \quad \frac{B}{A}(\rho) = \alpha\rho + \beta\rho^{\gamma}$$

	symmetric matter			neutron matter					
	α	β	γ	α	β	γ	$[\rho, B/A]_0$ (fm^{-3},MeV)	K (MeV)	E_{sym} (MeV)
V18 + UIX (G)	−452.5	556.0	1.24	78.0	232.9	2.24	[0.18, −15.3]	192	33.5
V18 + MICRO (G)	−123.2	407.9	2.38	55.9	532.3	2.68	[0.20, −14.7]	226	30.6
Bonn B + MICRO (G)	−130.4	537.0	2.39	31.0	780.2	2.77	[0.17, −15.9]	244	29.4
Nij93 + MICRO (G)	−152.5	343.3	1.94	72.3	693.6	2.67	[0.18, −15.4]	216	34.0
CD Bonn + UIX (K)	−306.5	424.0	1.38	87.3	175.0	2.33	[0.18, -15.56]	189.	34.5
V18 + UIX (K)	−265.5	406.0	1.47	77.1	257.4	2.27	[0.16, -15.98]	212.	31.9

Full dots : BHF calculations

Solid lines : polynomial fits

- UIX produce EoSes softer than microscopic TBF.
- G-matrix calculations give less repulsive B/A than the ones with K-matrix.
- Large uncertainty at high density.

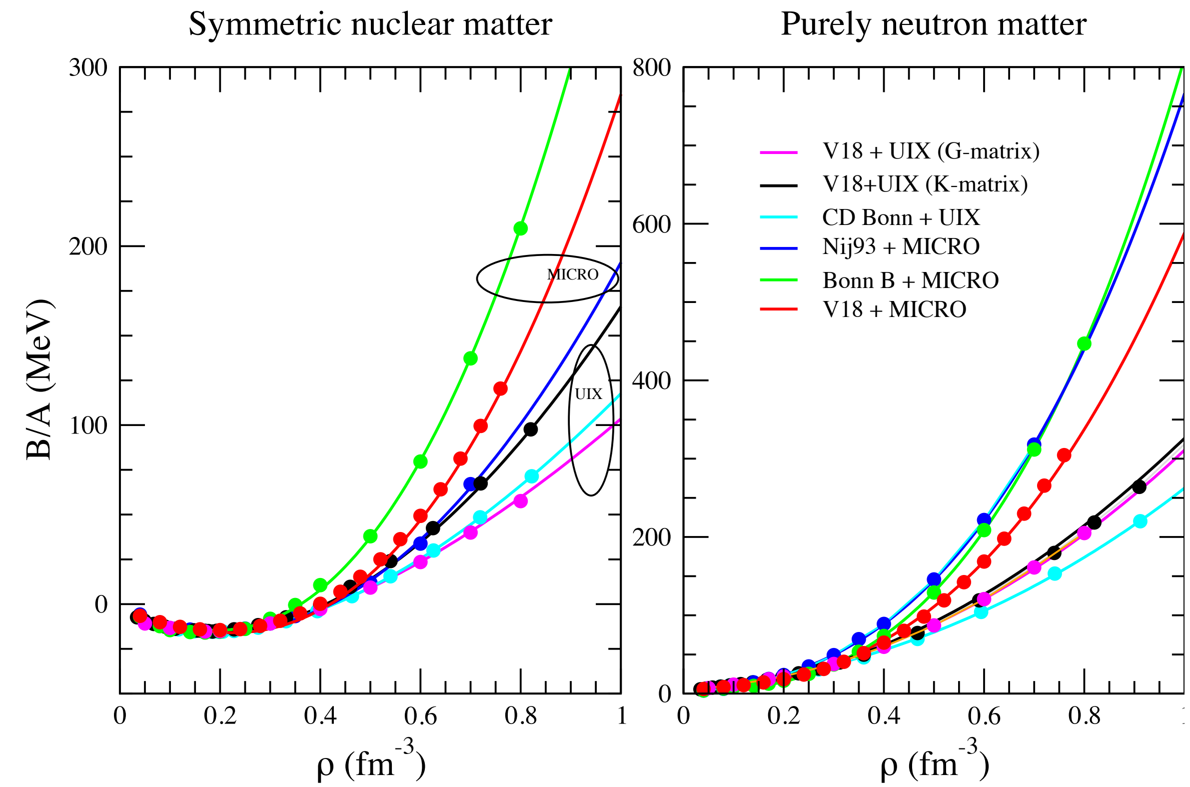

- More accurate fits at small density, in order to reproduce well the saturation point. Use of a different parametrization up to $\rho = 0.6\ fm^{-3}$

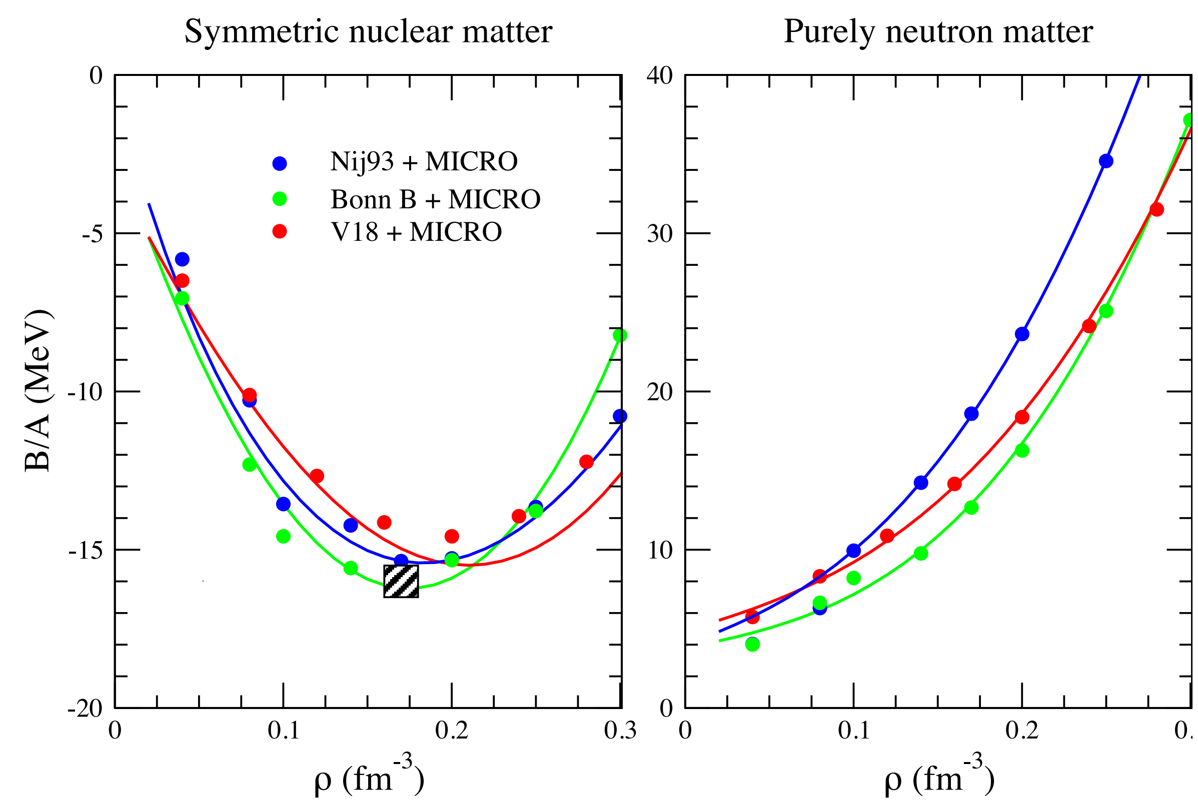

Micro +

Table 1. Parameters of the EOS for symmetric nuclear matter and pure neutron matter using different interactions.

	Symmetric matter				Neutron matter			
	a	b	c	d	a	b	c	d
Paris	−99.1	430.5	2.53	−3.19	33.7	644.7	2.87	4.78
Av18	−101.3	371.0	2.39	−3.12	32.5	585.7	2.73	4.87
Bonn B	−151.4	511.3	2.13	−2.21	21.8	814.0	2.83	3.79
Nij93	−242.6	385.7	1.52	−0.21	39.5	712.3	2.55	4.0

Including hyperons (Phys. Rev. C 84, 035801 (2011))

The basic input quantities are the NN, YN and YY potentials. The large number of degrees of freedom (four partial densities) renders inconvenient the use of the resulting hypernuclear Eos in tabular form ---> we tried to approximate the numerical results by a sufficiently accurate parametrization.

In the required range of nucleon densities $(0.1\ fm^{-3} \leq \rho_N \leq 0.8\ fm^{-3})$, proton fraction $(0 \leq \rho_p/\rho_N \leq 0.5\ fm^{-3})$ and hyperon fraction $(0 \leq \rho_\Sigma/\rho_N \leq 0.5\ fm^{-3}, 0 \leq \rho_\Lambda/\rho_N \leq 1.\ fm^{-3})$ an excellent fit of the energy density is given by :

$$\boxed{\begin{aligned}\varepsilon(\rho_n, \rho_p, \rho_\Lambda, \rho_\Sigma) &= E_N \rho_N \\ &+ (E_\Lambda + E_{\Lambda\Lambda} + E_{\Lambda\Sigma})\rho_\Lambda + \frac{C}{2m_\Lambda M_\Lambda}\rho_\Lambda^{5/3} \\ &+ (E_\Sigma + E_{\Sigma\Sigma} + E_{\Sigma\Lambda})\rho_\Sigma + \frac{C}{2m_\Sigma M_\Sigma}\rho_\Sigma^{5/3}\end{aligned}}$$

with

$$\left\{\begin{aligned} E_N &= (1-\beta)(a_0\rho_N + b_0\rho_N^{c0}) + \beta(a_1\rho_N + b_1\rho_N^{c1}), \\ E_Y &= (a_Y^0 + a_Y^1 x + a_Y^2 x^2)\rho_N + (b_Y^0 + b_Y^1 x + b_Y^2 x^2)\rho_N^{c_Y}, \\ E_{YY'} &= a_{YY'}\rho_N^{c_{YY'}}\rho_{Y'}^{d_{YY'}}, \\ M_Y &= 1 + (c_Y^0 + c_Y^1 x)\rho_N, \end{aligned}\right.$$

$$where \quad \rho_N = \rho_n + \rho_p, \quad x = \rho_p/\rho_N, \quad \beta = (1-2x)^2, \quad Y, Y' = \Lambda, \Sigma, \quad and \quad C = (3/5)(3\pi^2)^2/3 \approx 5.742$$

- All calculations performed with the G-matrix.
- Potentials used : V18 (NN), UIX and Micro (TBF's), NSC89 and ESC08 (NY). No YY.

TABLE I. Fit parameters for the energy density of hypernuclear matter, Eqs. (11) through (15), obtained with the ESC08 or the NSC89 YN potentials.

	V18 + TBF + ESC08							V18 + UIX′+ NSC89						
$a_0, b_0, c_0, a_1, b_1, c_1$	−140.7	390.1	2.08	88.3	634.3	3.11		−286.6	397.2	1.39	88.1	207.7	2.50	
$a^0_\Lambda, a^1_\Lambda, a^2_\Lambda, b^0_\Lambda, b^1_\Lambda, b^2_\Lambda, c_\Lambda$	−625	67	0	656	−17	0	1.28	−403	688	−943	659	−1273	1761	1.72
$a^0_\Sigma, a^1_\Sigma, a^2_\Sigma, b^0_\Sigma, b^1_\Sigma, b^2_\Sigma, c_\Sigma$	−1285	−395	0	1856	−93	0	1.07	−114	0	0	291	0	0	1.63
$a_{\Lambda\Lambda}, c_{\Lambda\Lambda}, d_{\Lambda\Lambda}$	218	0.95	0.84					136	0.51	0.93				
$a_{\Lambda\Sigma}, c_{\Lambda\Sigma}, d_{\Lambda\Sigma}$	0	0	0					0	0	0				
$a_{\Sigma\Sigma}, c_{\Sigma\Sigma}, d_{\Sigma\Sigma}$	0	0	0					0	0	0				
$a_{\Sigma\Lambda}, c_{\Sigma\Lambda}, d_{\Sigma\Lambda}$	157	0.95	0.80					89	0.33	0.81				
$c^0_\Lambda, c^1_\Lambda, c^0_\Sigma, c^1_\Sigma$	−0.13	1.76	−0.75	−0.44				0.22	−0.38	−0.59	−0.22			

Main differences :

- ✓ ( ) more repulsive (attractive) in ESC08 than in NSC89

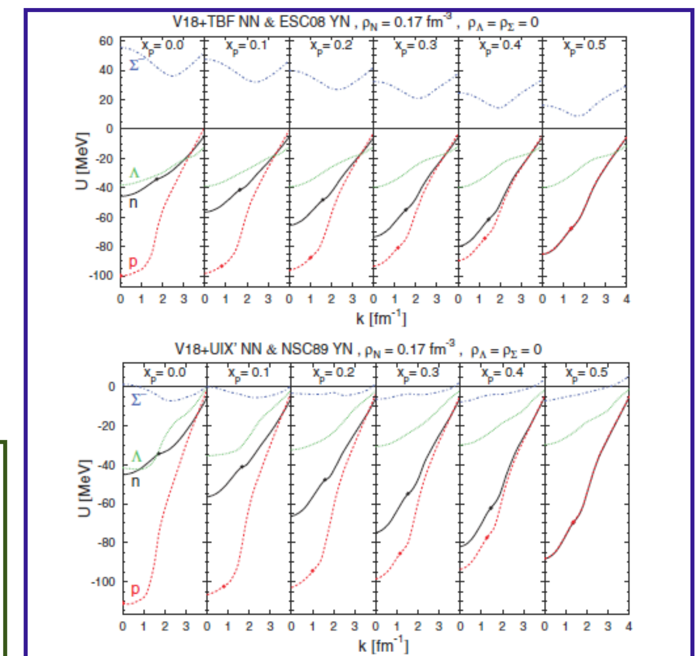

- ✓ Swap in the composition
- ✓ No change in the EoS

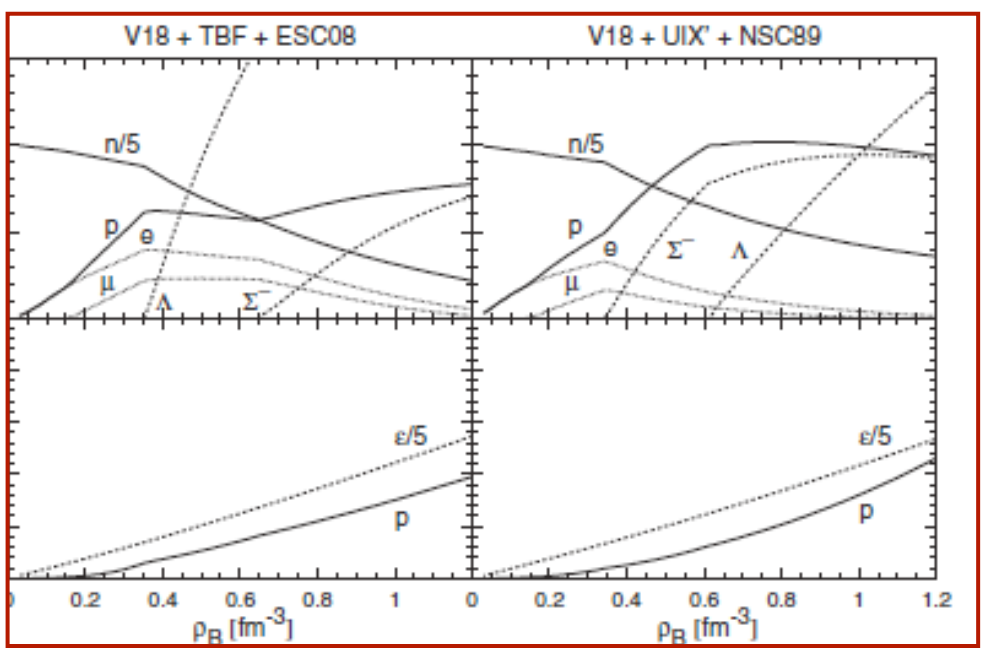

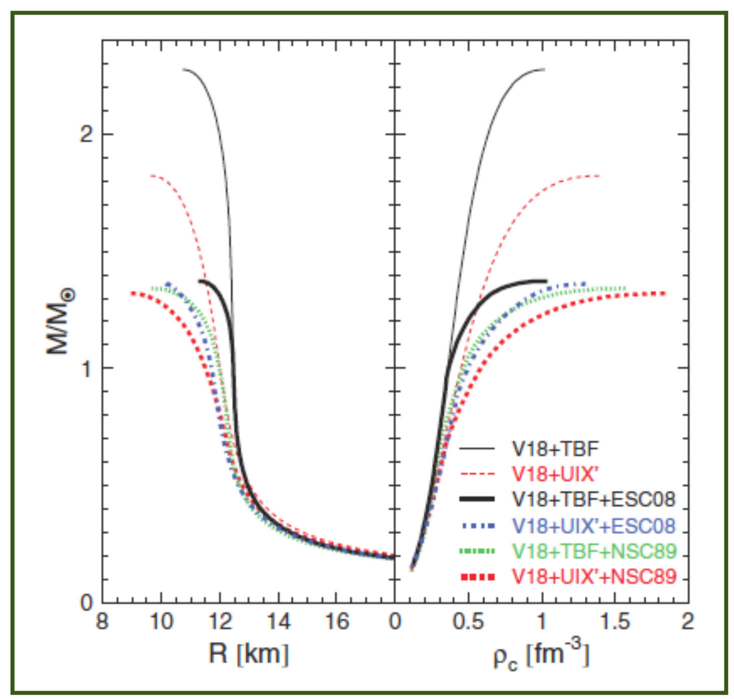

TABLE I. Fit parameters for the energy density of hypernuclear matter, Eqs. (11) through (15), obtained with the ESC08 or the NSC89 YN potentials.

	V18 + TBF + ESC08							V18 + UIX′+ NSC89						
$a_0, b_0, c_0, a_1, b_1, c_1$	−140.7	390.1	2.08	88.3	634.3	3.11		−286.6	397.2	1.39	88.1	207.7	2.50	
$a_\Lambda^0, a_\Lambda^1, a_\Lambda^2, b_\Lambda^0, b_\Lambda^1, b_\Lambda^2, c_\Lambda$	−625	67	0	656	−17	0	1.28	−403	688	−943	659	−1273	1761	1.72
$a_\Sigma^0, a_\Sigma^1, a_\Sigma^2, b_\Sigma^0, b_\Sigma^1, b_\Sigma^2, c_\Sigma$	−1285	−395	0	1856	−93	0	1.07	−114	0	0	291	0	0	1.63
$a_{\Lambda\Lambda}, c_{\Lambda\Lambda}, d_{\Lambda\Lambda}$	218	0.95	0.84					136	0.51	0.93				
$a_{\Lambda\Sigma}, c_{\Lambda\Sigma}, d_{\Lambda\Sigma}$	0	0	0					0	0	0				
$a_{\Sigma\Sigma}, c_{\Sigma\Sigma}, d_{\Sigma\Sigma}$	0	0	0					0	0	0				
$a_{\Sigma\Lambda}, c_{\Sigma\Lambda}, d_{\Sigma\Lambda}$	157	0.95	0.80					89	0.33	0.81				
$c_\Lambda^0, c_\Lambda^1, c_\Sigma^0, c_\Sigma^1$	−0.13	1.76	−0.75	−0.44				0.22	−0.38	−0.59	−0.22			

Main differences :

- ✓ $\Sigma^-(\Lambda)$ more repulsive (attractive) in ESC08 than in NSC89

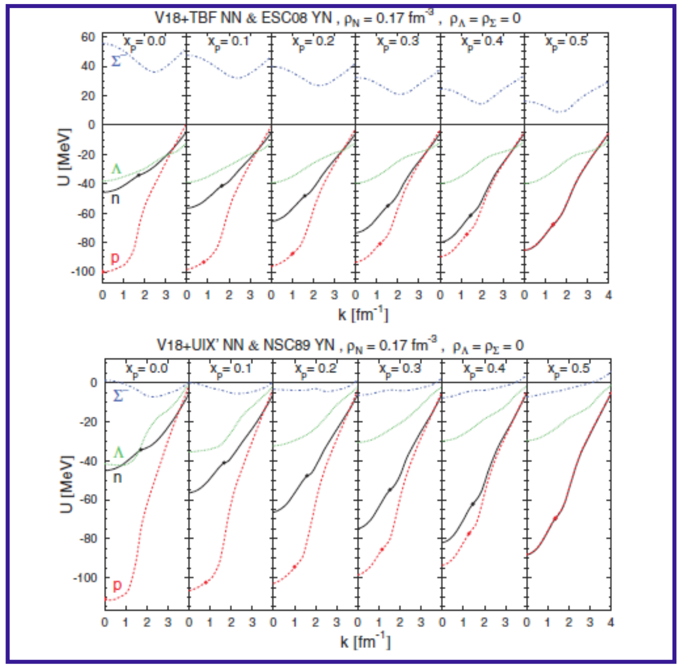

- ✓ Swap in the composition
- ✓ No change in the EoS

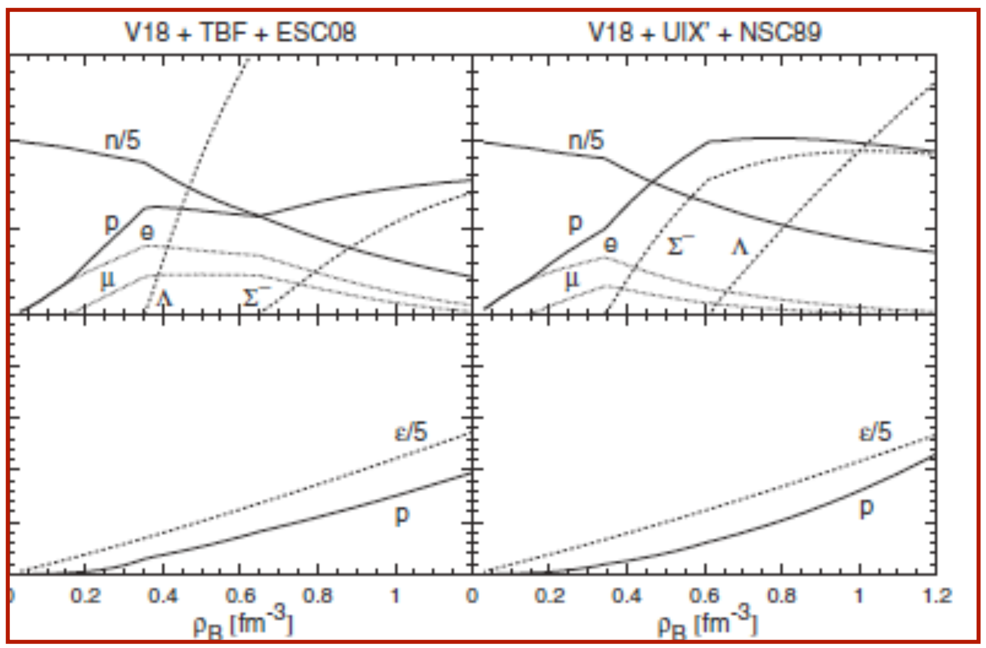

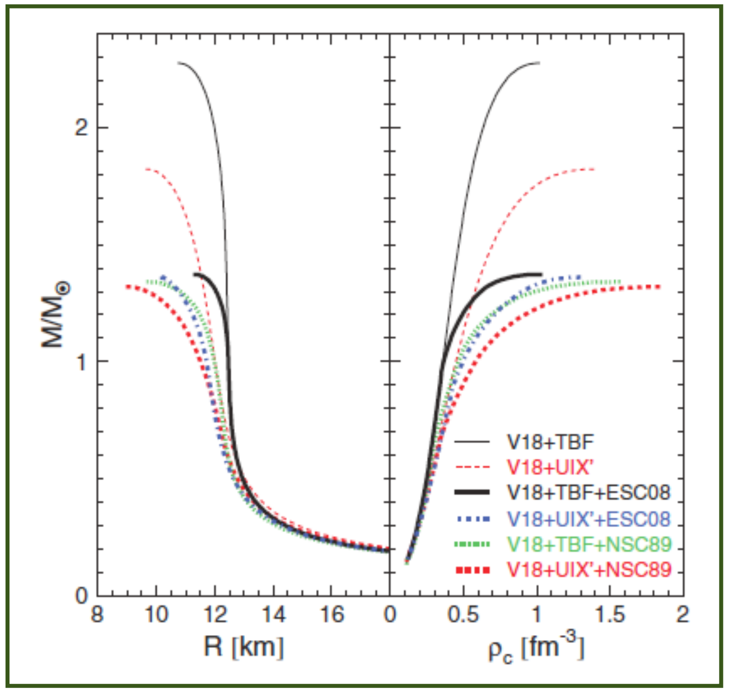

Case b) : T≠0

The Bloch-De Dominicis theory of nuclear matter

$$\Omega = \Omega_0' + \Delta\Omega$$

$$\Omega_0' = -\frac{2V}{\pi^2}\int_0^\infty k^2 dk\left[\frac{1}{\beta}\log(1+e^{-\beta(E_k-\mu)}) + U(k)n(k)\right]$$

$$U(k_1) = \sum_{k_2} n(k_2) < k_1k_2|K(W)|k_1k_2 >_A$$

$$< k_1k_2|K(W)|k_3k_4 > \; = \; < k_1k_2|V|k_3k_4 > + \mathrm{Re}\sum_{k_3'k_4'} < k_1k_2|V|k_3'k_4' > \frac{[1-n(k_3')][1-n(k_4')]}{W-E_{k_3'}-E_{k_4'}+i\epsilon} < k_3'k_4'|K(W)|k_3k_4 >$$

$$\Delta\Omega = \frac{1}{2}e^{2\beta\mu}\int_{-\infty}^{\infty} d\omega \frac{e^{-\beta\omega}}{2\pi}\mathrm{Tr}_2\left[arctan\left(\mathcal{K}(\omega)\pi\delta(H_0-\omega)\right)\right]$$

$$< k_1k_2|\mathcal{K}(\omega)|k_3k_4 > = < k_1k_2|K(\omega)|k_3k_4 > \prod_{i=1,4}\sqrt{1-n_i(k)}$$

Thermodynamics of the hadronic phase :

$$s = -\frac{\partial f}{\partial T} \qquad f = \Omega + \rho\mu \qquad \epsilon = f + Ts \qquad P = \rho^2\left(\frac{\partial(f/\rho)}{\partial\rho}\right)_T$$

EoS at finite T for symmetric nuclear matter

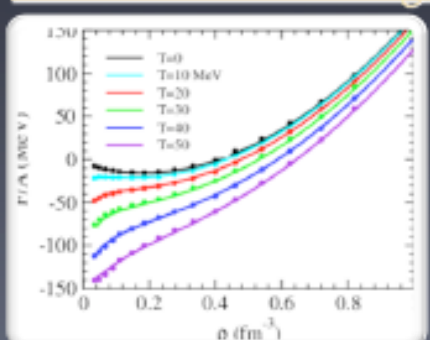

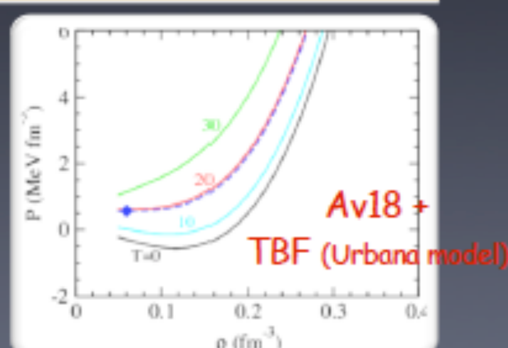

Typical Van der Waals behavior, with T_c=20 MeV and ρ_c~0.06 fm^{-3}

The critical point depends on the many-body method and the NN interaction

- Calculations performed for the K-matrix
- The free energy density :

$$\boxed{f_{NN} = \sum_{i=n,p}\left[2\sum_k n_i(k)\left(\frac{k^2}{2m_i}+\frac{1}{2}U_i(k)\right) - Ts_i\right]}$$

with $s_i = -2\sum_k \left(n_i(k)\ln n_i(k) + [1-n_i(k)]\ln[1-n_i(k)]\right)$

- Argonne V18 + UIX as input

We find that the following functional forms provide excellent parametrizations of the new numerical results in the required ranges of density (0.03 fm^{-3} $\lesssim \rho \lesssim$ 1 fm^{-3}) and temperature (0 MeV $\le T \le$ 50 MeV) for symmetric (SNM) and pure neutron matter (PNM):

$$\frac{F}{A}(T,\rho) = -(137+157t^2)\rho + 308\rho^{1.82} + 207t^2\ln(\rho) + (-47.5t^2+71t^{2.41})/\rho - 5 \qquad \text{(SNM)},$$

$$\frac{F}{A}(T,\rho) = (11-122t^2)\rho + 309\rho^{1.95} + 173t^2\ln(\rho) + (-48t^2+71t^{2.35})/\rho + 6 \qquad \text{(PNM)},$$

where $t = T/(100\text{ MeV})$ and F and ρ are given in MeV and fm^{-3}, respectively.

- Parabolic approx. holds true also @T≠0

$$\frac{F}{A}(T,\rho,x) \approx \frac{F}{A}(T,\rho,x=0.5) + (1-2x)^2 F_{sym}(T,\rho),$$

- Extension to G-matrix, more time consuming !
- Frozen Correlations Approximation : at T≠0 correlations are almost the same as @ T=0.
- Calculations performed with Argonne v18 + UIX and Micro TBF's

$$\frac{E}{A}(\rho, T) = (a_1 t + a_2 t^2) + (b_0 + b_1 t)\rho + (c_0 + c_1 t)\rho^d,$$

$$\frac{F}{A}(\rho, T) = (a_1 t + a_2 t^2)\ln(\rho) + (b_0 + b_2 t^2)\rho + c_0 \rho^d,$$

where $t = T/(100\ \mathrm{MeV})$ and E, F, and ρ are given in MeV and fm^{-3}, respectively. The parameters of the different fits are reported in Table I for both TBFs that we use.

TABLE I. Parameters of EOS fits, Eqs. (10) and (11), for symmetric nuclear matter (SNM) and pure neutron matter (PNM), with both nuclear TBFs used.

	a_1	a_2	b_0	b_1	b_2	c_0	c_1	d
Micro-TBF								
E/A, SNM	81	95	−155	−139		395	81	2.09
E/A, PNM	101	73	54	−181		659	84	2.88
F/A, SNM	41	120	−115		−182	355		2.24
F/A, PNM	18	123	83		−103	631		3.02
Pheno-TBF								
E/A, SNM	105	74	−473	−464		586	381	1.26
E/A, PNM	109	64	34	−240		249	164	1.97
F/A, SNM	41	116	−180		−174	293		1.57
F/A, PNM	21	116	101		−131	191		2.62

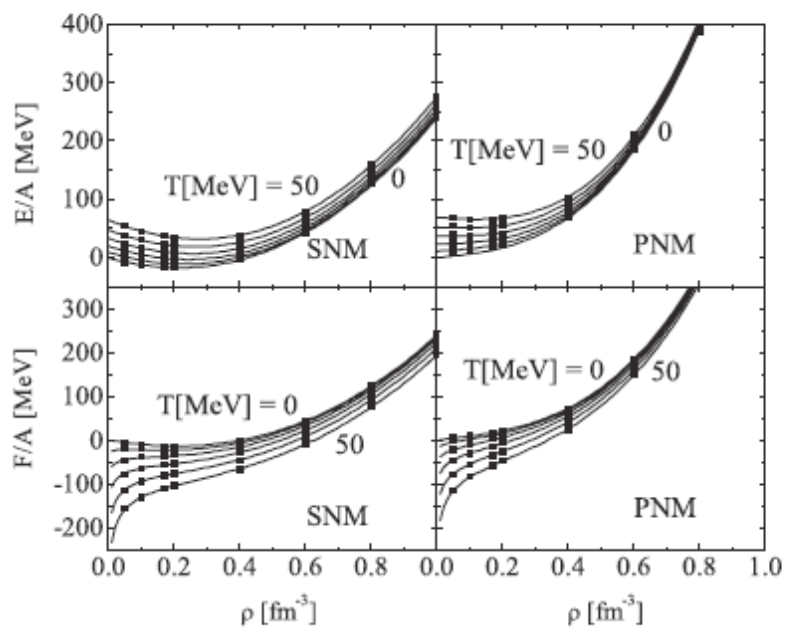

FIG. 1. Finite-temperature EOS for symmetric (left panels) and purely neutron (right panels) matter. The internal energy (upper panels) and the free energy (lower panels) are displayed as a function of the nucleon density, for temperatures ranging from 0 to 50 MeV, in steps of 10 MeV. Numerical data (symbols) and results of the fits, Eqs. (10) and (11) (curves), are shown.

Including hyperons at finite T

- Calculations with : G-matrix plus Argonne v18, UIX TBF's, and NSC89 NY potentials
- Use of the Frozen Correlations Approximation.
- Only Σ^- and Λ hyperons.

$$f(\rho_n, \rho_p, \rho_\Lambda, \rho_\Sigma, T) = F_N \rho_N + (F_\Lambda + F_{\Lambda\Lambda} + F_{\Lambda\Sigma})\rho_\Lambda + \frac{C}{2m_\Lambda M_\Lambda}\rho_\Lambda^{5/3} + (F_\Sigma + F_{\Sigma\Sigma} + F_{\Sigma\Lambda})\rho_\Sigma + \frac{C}{2m_\Sigma M_\Sigma}\rho_\Sigma^{5/3}$$

with the parametrizations at zero temperature:

$$F_N = (1-\beta)(a_0\rho_N + b_0\rho_N^{c_0}) + \beta(a_1\rho_N + b_1\rho_N^{c_1}),$$
$$F_Y = (a_Y^0 + a_Y^1 x + a_Y^2 x^2)\rho_N + (b_Y^0 + b_Y^1 x + b_Y^2 x^2)\rho_N^{c_Y},$$

$$F_{YY'} = a_{YY'}\rho_N^{c_{YY'}}\rho_{Y'}^{d_{YY'}},$$
$$M_Y = 1 + (c_Y^0 + c_Y^1 x)\rho_N,$$

where $\rho_N = \rho_n + \rho_p$; $x = \rho_p/\rho_N$; $\beta = (1-2x)^2$; $Y, Y' = \Lambda, \Sigma$, and $C = (3/5)(3\pi^2)^{2/3} \approx 5.742$. At finite temperature the expressions are extended as follows:

$$F_N = F_N(T=0) + [\tilde{a}_0 t^2\rho_N + (\tilde{d}_0 t^2 + \tilde{e}_0 t^3)\ln(\rho_N) + \tilde{f}_0 t^2/\rho_N](1-\beta) + [\tilde{a}_1 t^2\rho_N + (\tilde{d}_1 t^2 + \tilde{e}_1 t^3)\ln(\rho_N) + \tilde{f}_1 t^2/\rho_N]\beta,$$
$$F_Y = F_Y(T=0) + (\tilde{d}_Y t^2 + \tilde{e}_Y t^1)\ln(\rho_N) + \tilde{f}_Y t^2/\rho_N + \tilde{g}_Y t^2\ln(\rho_Y),$$

$$M_Y = M_Y(T=0) + \tilde{b}_Y t^2\rho_N^{\tilde{c}_Y},$$

where $t = T/(100\ \text{MeV})$ and f and ρ_i are given in MeV fm^{-3} and fm^{-3}, respectively (and $m_{\Lambda,\Sigma}$ in MeV^{-1} fm^{-2}).

TABLE I. Fit parameters for the free energy density, Eqs. (12)–(19).

$a_0, b_0, c_0, a_1, b_1, c_1$	−286.6	397.2	1.39	88.1	207.7	2.50	
$a_\Lambda^0, a_\Lambda^1, a_\Lambda^2, b_\Lambda^0, b_\Lambda^1, b_\Lambda^2, c_\Lambda$	−403	688	−943	659	−1273	1761	1.72
$a_\Sigma^0, a_\Sigma^1, a_\Sigma^2, b_\Sigma^0, b_\Sigma^1, b_\Sigma^2, c_\Sigma$	−114	0	0	291	0	0	1.63
$a_{\Lambda\Lambda}, c_{\Lambda\Lambda}, d_{\Lambda\Lambda}$	136	0.51	0.93				
$a_{\Lambda\Sigma}, c_{\Lambda\Sigma}, d_{\Lambda\Sigma}$	0	0	0				
$a_{\Sigma\Sigma}, c_{\Sigma\Sigma}, d_{\Sigma\Sigma}$	0	0	0				
$a_{\Sigma\Lambda}, c_{\Sigma\Lambda}, d_{\Sigma\Lambda}$	89	0.33	0.81				
$c_\Lambda^0, c_\Lambda^1, c_\Sigma^0, c_\Sigma^1$	0.22	−0.38	−0.59	−0.22			
$\tilde{a}_0, \tilde{d}_0, \tilde{e}_0, \tilde{f}_0$	−202.0	396.9	−190.6	35.2			
$\tilde{a}_1, \tilde{d}_1, \tilde{e}_1, \tilde{f}_1$	−138.0	308.4	−109.3	31.2			
$\tilde{d}_\Lambda, \tilde{e}_\Lambda, \tilde{f}_\Lambda, \tilde{g}_\Lambda, \tilde{b}_\Lambda, \tilde{c}_\Lambda$	92.3	29.3	39.4	152.3	4.78	3.95	
$\tilde{d}_\Sigma, \tilde{e}_\Sigma, \tilde{f}_\Sigma, \tilde{g}_\Sigma, \tilde{b}_\Sigma, \tilde{c}_\Sigma$	89.2	61.0	63.6	186.8	1.13	3.30	

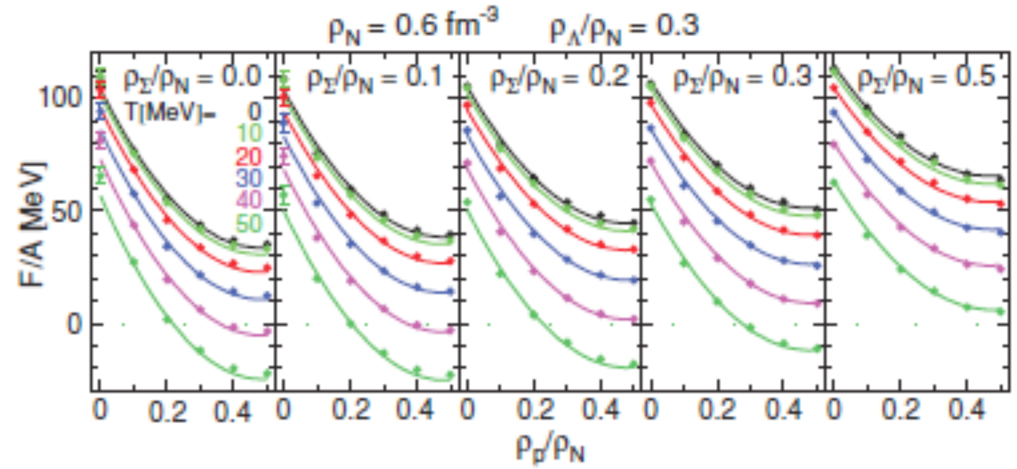

FIG. 1. (Color online) Free energy per baryon, F/A, at fixed nucleon density $\rho_N = 0.6$ fm^{-3} and lambda fraction $\rho_\Lambda/\rho_N = 0.3$, as a function of proton fraction $\rho_p/\rho_N = 0, \ldots, 0.5$ and sigma fraction $\rho_\Sigma/\rho_N = 0, 0.1, 0.2, 0.3, 0.5$ for different temperatures $T = 0, 10, \ldots, 50$ MeV. BHF data (symbols) and fit (curves) are shown.

EoS of the inner crust

M. Baldo, E.E. Saperstein, S.V. Tolokonnikov,
Nucl. Phys. A **775**, 235 (2006).
Eur. Phys. J. A **32**, 97 (2007).
Phys. Rev. C **76**, 025803 (2007).

- Wigner-Seitz method
- Generalized EDF Method (DF3 functional by Fayans)
- Inclusion of neutron and proton pairing correlations
- Neutron drip point same as in BPS and NV approaches
- Slightly different crust composition

k_F (fm^{-1})	Z	Z [3]	A	A [3]	R_c (fm)	R_c (fm) [3]	x	x [3]
0.2	52	40	212	180	57.2	53.6	0.245	0.222
0.3	54	40	562	320	52.8	44.3	0.096	0.125
0.4	50	40	830	500	45.1	42.2	0.060	0.080
0.5	46	40	1020	950	38.6	39.3	0.045	0.042

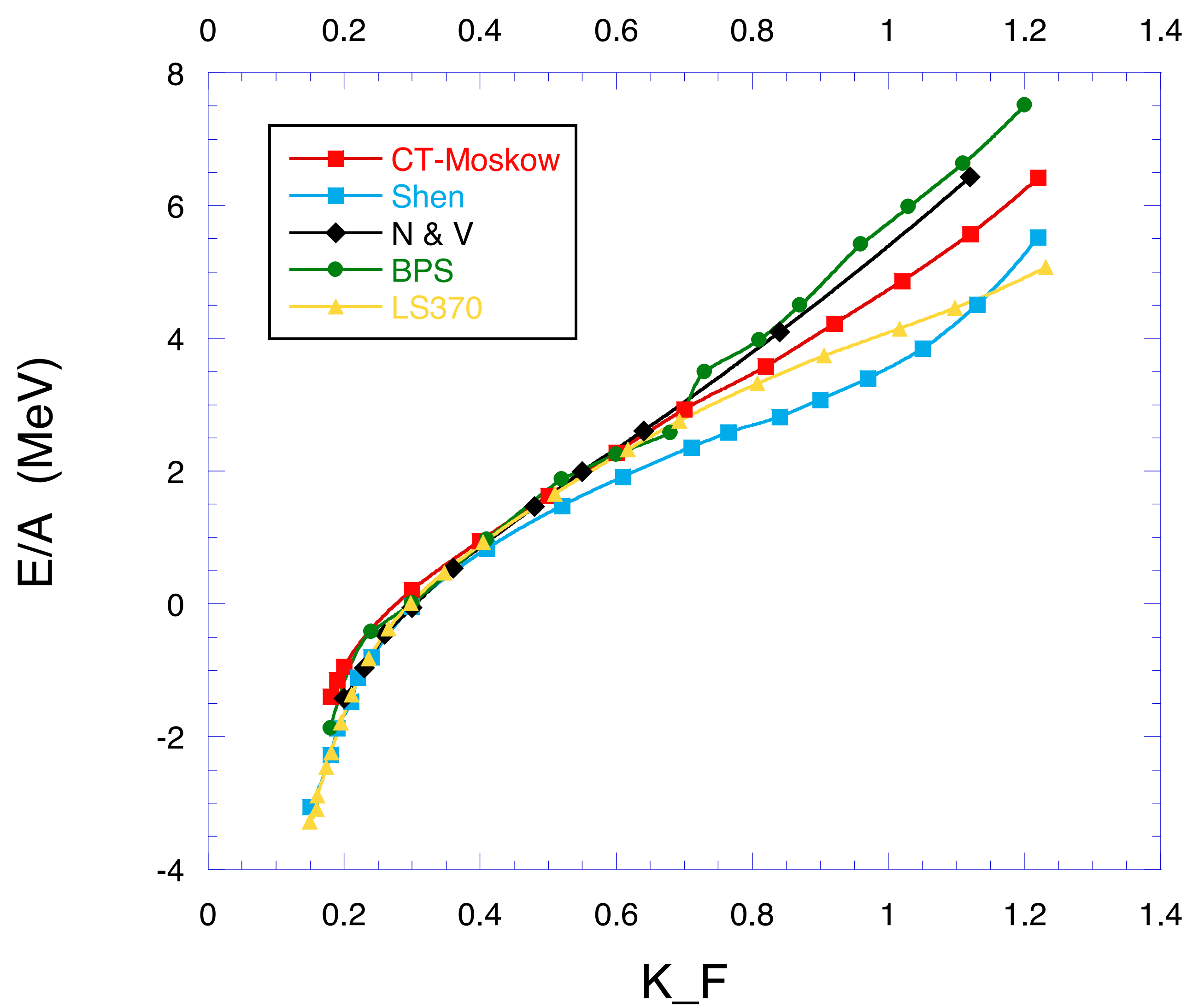

- Negligible effects of pairing on the EoS.

Fitted by :

$$\frac{E}{A} = -4.58 + 23.44\ k_F - 33.46\ k_F^2 + 27.2\ k_F^3 - 7.7\ k_F^4$$

Nucleon effective masses m*

$$\frac{m^*(k;\rho)}{m} = \frac{k}{m}\left[\frac{de(k;\rho)}{dk}\right]^{-1}$$

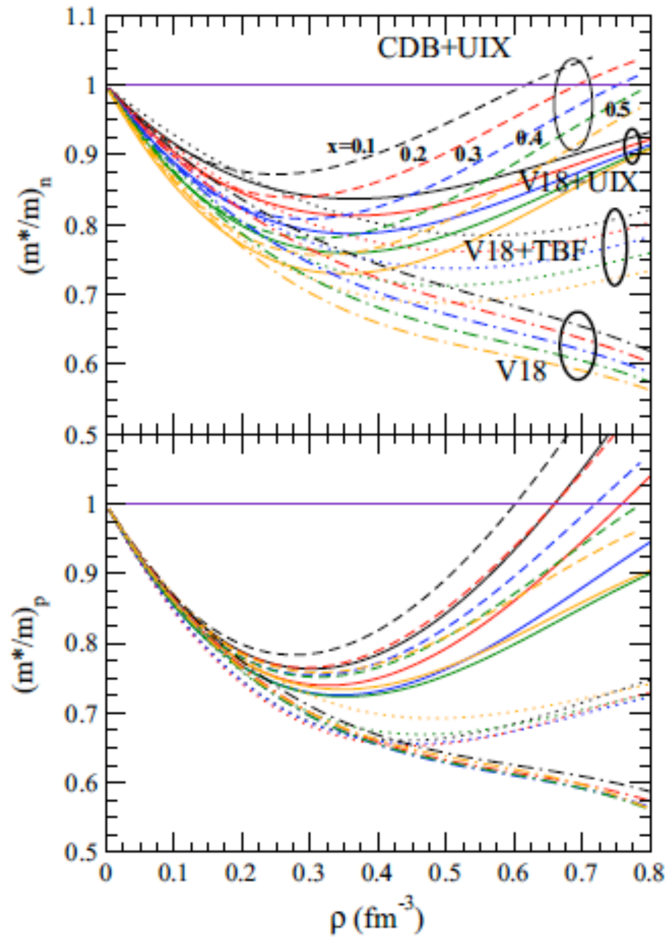

FIG. 1. (Color online) Neutron (top) and proton (bottom) effective mass displayed vs the nucleon density for several values of the proton fraction: $x = 0.1, 0.2, 0.3, 0.4$, and 0.5. Results are plotted for different choices of two- and three-body forces, as discussed in the text.

$$\frac{m^*}{m}(\rho,x) = 1-(a_1+b_1x+c_1x^2)\rho + (a_2+b_2x+c_2x^2)\rho^2 - (a_3+b_3x+c_3x^2)\rho^3,$$

TABLE I. Parameters of the polynomial fits, Eq. (6), for the neutron and proton effective masses, obtained with different interactions. The density ρ is understood in units of fm^{-3} with these coefficients.

	a_1	b_1	c_1	a_2	b_2	c_2	a_3	b_3	c_3
V18									
p	1.45	0.85	−0.92	2.10	1.26	−0.44	1.13	0.65	0.42
n	0.96	0.92	0.59	1.20	1.38	1.64	0.71	0.65	0.98
V18 + TBF									
p	1.67	0.99	−2.47	2.70	1.18	−3.75	1.14	0.88	−2.40
n	0.61	1.55	0.91	0.42	2.01	4.77	−0.17	0.58	4.44
V18 + UIX									
p	1.56	1.31	−1.89	3.17	1.26	−1.56	0.79	3.78	−3.81
n	0.88	1.21	1.07	1.64	2.06	2.87	0.78	0.98	1.62
CDB + UIX									
p	1.53	0.80	−1.04	3.05	1.06	−1.44	0.43	4.04	−4.42
n	0.95	1.17	0.42	2.44	1.27	−0.05	1.30	0.55	−1.63

Bibliography

EoS of the core

Z.H. Li and H.-J. Schulze, PRC **78**, 028801 (2008)
A. Li, X. R. Zhou, G.F. Burgio and H.-J. Schulze PRC **81** , 025806 (2010)
G.F. Burgio and H.-J. Schulze, *A&A* **518**, A17 (2010)
G.F. Burgio, A. Li and H.-J. Schulze, PRC **83**, 025804 (2011)
H.-J. Schulze and T. Rjiken, PRC **84**, 035801 (2011)
Z.H.Li, D.P. Zhang, H.-J. Schulze and W. Zuo, Chin. Phys. Lett. **29**, 012101(2012)

Nucleon effective masses

M. Baldo, G.F. Burgio, H.-J. Schulze and G. Taranto, PRC **89**, 048801 (2014)

EoS of the crust

M. Baldo, E. Saperstein and S. Tolonnikov, PRC **76**, 025803 (2007)